Chapter 6

Improvements of Brightness of a-SiC:H TFLEDs

6.1 Introduction

In this works, the author has succeeded in the fabrication of amorphous visible-light thin film light emitting diodes (TFLEDs) from several amorphous silicon alloys, so-called, a-SiN:H, a-SiC:H and a-SiO:H [1-3]. The devices gather attentions because they have possibilities to be used as new types of flat panel displays. However, the main drawback of the devices is the low brightness. Therefore, it is necessary to improve more the brightness of the device.

In these few years, there have been several groups who tried to improve the brightness. For example, the group of National Central University, Taiwan, used a quantum well injection structure in the TFLED [4]. The group of University College of Swansea, UK, prepared p-microcrystalline-SiC:H layer by using laser annealing of p-a-SiC:H [5]. The group of Osaka University, Japan, used a hot carrier injection structure [6]. However, the brightnesses were still several cd/m^2 which are still too low for a flat panel display which requires more than 50 cd/m^2.

The main concepts to improve the brightness of a TFLED are 1) to improve the radiative recombination efficiency and 2) to improve the carrier injection efficiency.

In this work, efforts have been made to improve the brightness of amorphous TFLEDs by using two new methods as follows:

1. Improve the radiative recombination efficiency by using metal sheets as substrates instead of conventional glass substrates. A thermal conductivity of a sheet metal substrate is higher than that of a glass substrate. Therefore, the heat dissipation from the TFLED deposited on a metal sheet substrate should be better than the case in which a glass substrate is used [7-8]. By this technique the brightness has been increased by a factor of 2-5 to the level of 5 cd/m^2.

2. Improve the carrier (holes) injection efficiency by using boron doped wide gap and highly conductive a-SiO:H and μC-SiO:H materials as the hole injection layer [3]. The result shows that by using this technique the brightness has been increased to the level of 10 cd/m^2. This value is the best record reported so far. Discussion will be done on the mechanism of the tunnelling injection of holes through the barrier at the p/i interfaces.

In this chapter, the focus will be placed on the a-SiC:H p-i-n TFLEDs.

6.2 Improvement of Brightness by Using Metal Substrates

One factor that limits the brightness of a LED is the thermal quenching effect of the internal luminescent quantum efficiency due to the bad thermal conductivity of the substrate. In the case of the amorphous TFLED, all of the reports use a sheet of glass as a substrate so far. Therefore, the heat generated in the p-i-n junctions during operation can not dissipate to the substrate, this results in the increase in the temperature of the p-i-n junctions and eventually decreases the external luminescent quantum efficiency of the device. In this work, a new idea is to use metal substrate so that the heat dissipation should be efficient and therefore the temperature of the p-i-n junctions will decrease quickly.

6.2.1 Advantages of Metal Substrates for Amorphous TFLEDs

A metal substrate has not only a good heat dissipation property but also has various advantages to be used for an amorphous TFLED as follows:

(1) Strength material.

(2) During the injection of electrical current into the TFLED, heat may cause glass substrate to crack, while metal sheet substrate will not crack. Figure 6.1 shows an example of the crack (break) of a glass substrate due to the heat generated in the amorphous TFLED.

(3) A thermal conductivity of metal is higher than that of glass. Therefore, the heat dissipation from the TFLED deposited on a metal substrate should be better than the case in which a glass substrate is used. Therefore, the external quantum

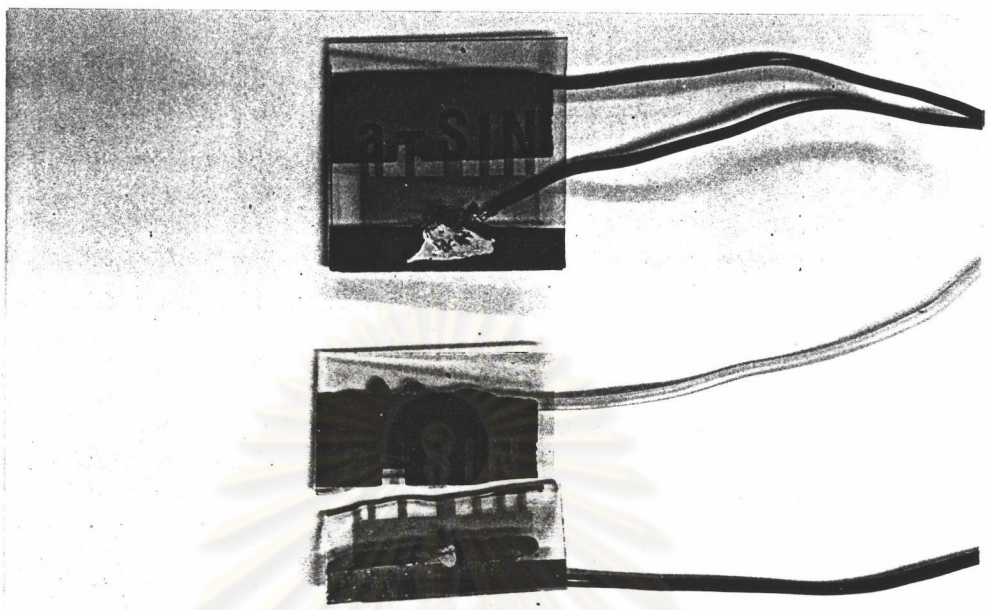

Figure 6.1 Example of breaking of a glass substrate due to heat generated in an amorphous TFLED.

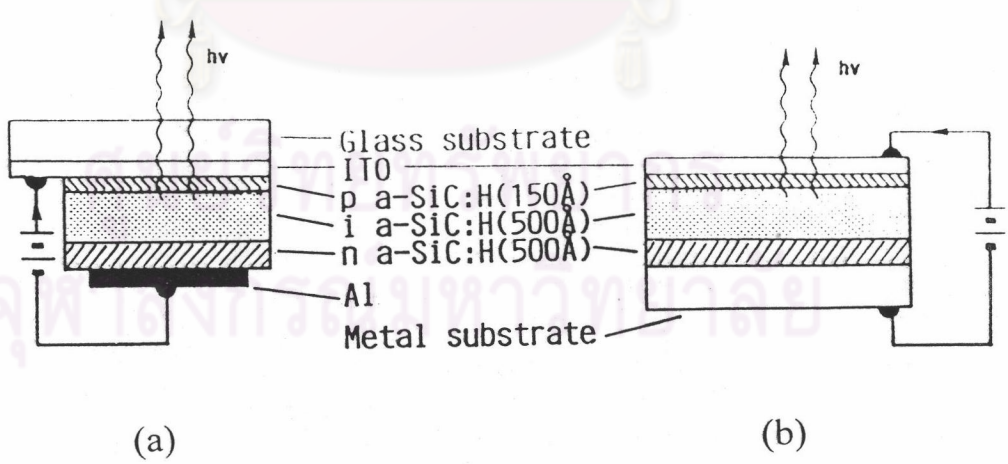

Figure 6.2 Schematic illustrations of the structures of the a-SiC:H TFLED with (a) glass substrate and (b) metal substrate.

efficiency of luminescence for the device having metal sheet as a substrate should be better than the case of having glass as a substrate. This case leads to a brighter and perhaps more stable TFLED.

(4) The TFLED having metal sheet as a substrate which naturally acts a heat sink can be easily connected to a cooler, for example a thermo-electric cooler, so that the temperature of the TFLED during operation can be controlled. Keeping the device at low temperature will lead to a brighter emission from the device.

(5) The surface of smooth metal sheet is normally lustrous like mirror surface. The mirror surface will act as a good reflection of the generated light. This will lead to a brighter device.

(6) A metal sheet is normally flexible. Therefore, a new type of flexible TFLED flat panel display can be realized.

(7) A metal sheet substrate itself can be also act as an electrode for the TFLED. This will lead to a reduction in the cost and time for the production process.

6.2.2 Structure and Fabrication of a-SiC:H TFLED Using Metal Substrate

Figure 6.2 shows a comparison between the structures of the a-SiC:H TFLEDs with (a) a glass substrate and (b) a metal substrate. The proposed structure is metal substrate/ n-a-SiC:H/ i-a-SiC:H/ p-a-SiC:H/ITO. The a-SiC:H p-i-n layers were prepared by the glow discharge plasma CVD system. The thicknesses of the p-i-n layers are the same as mentioned in other chapters, so-called 150 Å, 500 Å and 500 Å, respectively. It is noted that the top layer where light comes out in both types (a) & (b) is basically the p-layer. The ITO electrode was deposited by an electron beam (EB) evaporator at the substrate temperature of 250 °C. The optical energy gaps of p-, i- and n-layers for the experiment in this chapter were chosen to be 2.0, 3.0 and 2.0 eV, respectively. The observation of emission in device (b) is done through the top transparent ITO electrode. The details of the preparation conditions of a-SiC:H p-i-n junctions have been reported in chapters 2 and 4.

In this work, several kinds of metal sheets having different surface roughnesses for example, SUS (stainless steel), Cu (copper), Al (aluminum), Zn (zinc)

and bronze have been examined as substrates. The thickness of the metal sheet is about 0.5 - 1.0 mm.

6.2.3 Characteristics of a-SiC:H TFLED with Metal Substrate

In this work the first examination has been done to check that what kind of metal material can be used as a substrate. The metal materials were for example SUS, Cu, Al, Zn and Bronze. It was found that the all of these metals can be used but what is more important is that the roughness of the surface of the material must not be more than 0.1 μm. Figure 6.3 shows the comparison of the I-V curves for the TFLEDs deposited on stainless steel substrates with different roughness of surface. It was found that the I-V curve for the TFLED deposited on the substrate with surface roughness more than 0.1 micron can not show a good diode characteristic. The condition of the smoothness of the surface of the metal substrate for the amorphous TFLED seems to be severer than in the case for a-Si:H solar cell. .

Figure 6.4 shows the comparisons of the brightnesses of a-SiC:H TFLEDs deposited on glass substrates and on SUS substrates. The area of each device is 15 mm^2. As the optical energy gap increases, the brightness of both the cases of glass and SUS substrates increases. It is clear that at the same optical energy gap of the i-layer, the brightness for SUS substrate is always higher than that for glass substrate by a factor of 2-5. The maximum brightness of 5 cd/m^2 was obtained in the yellow a-SiC:H TFLED of which the optical energy gap of the i-layer is 3.0 eV.

The maximum injection current density used in Fig. 6.4 was as high as 1000 mA/cm^2. This current density might be very high for the practical display. Therefore, in the practical use, it is recommended in the thesis that maximum injection current density should be about the order of 100 mA/cm^2 to ensure a good stability, long life time and low power consumption.

The emission spectrum of a-SiC:H TFLED (E_{opt} of i-layer = 3.0 eV) deposited on a SUS substrate shows a broad band peaking at around 650 nm as shown in Fig. 6.5. The device exhibits an orange-red color emission.

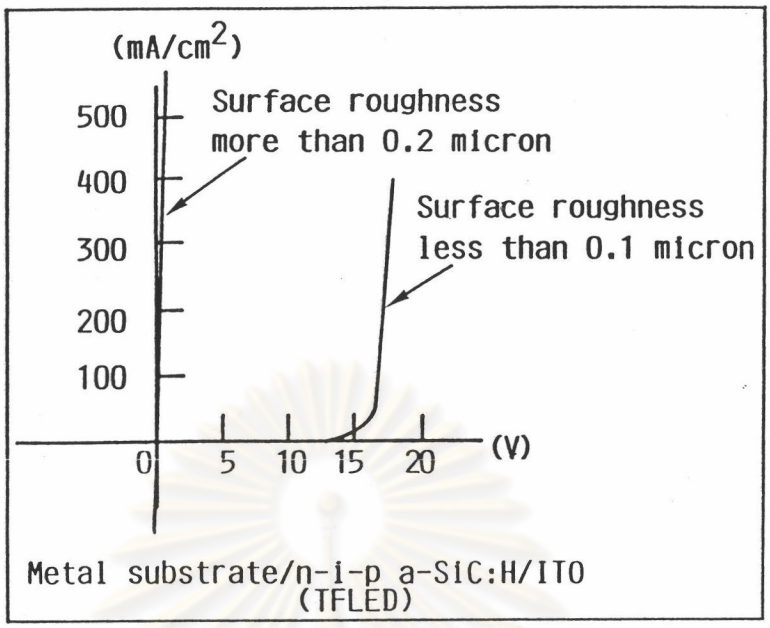

Figure 6.3 Comparison of the I-V curves for the a-SiC:H TFLEDs deposited on stainless steel substrates with different roughness of the surface.

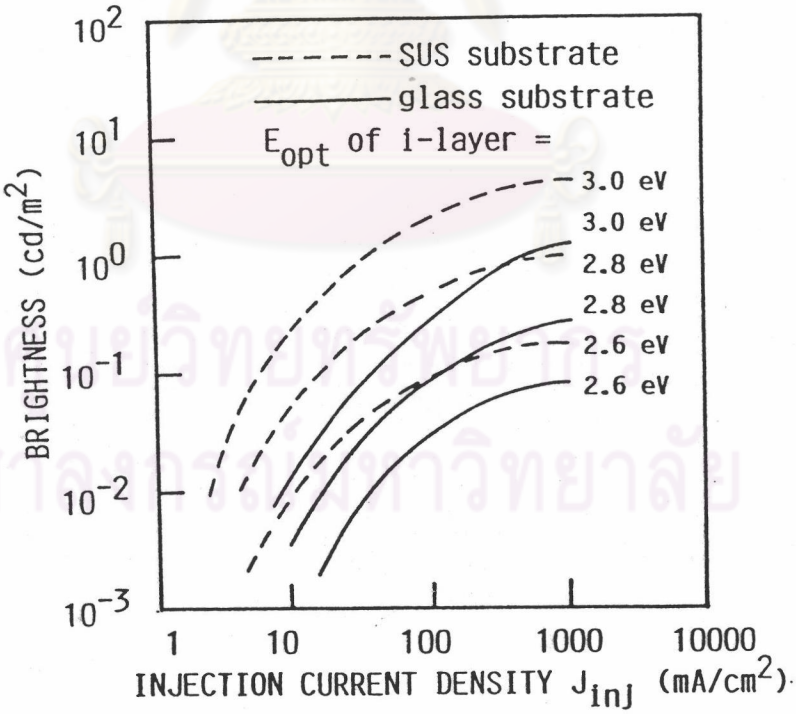

Figure 6.4 Comparisons of the brightnesses of a-SiC:H TFLEDs deposited on glass substrates and on SUS substrates.

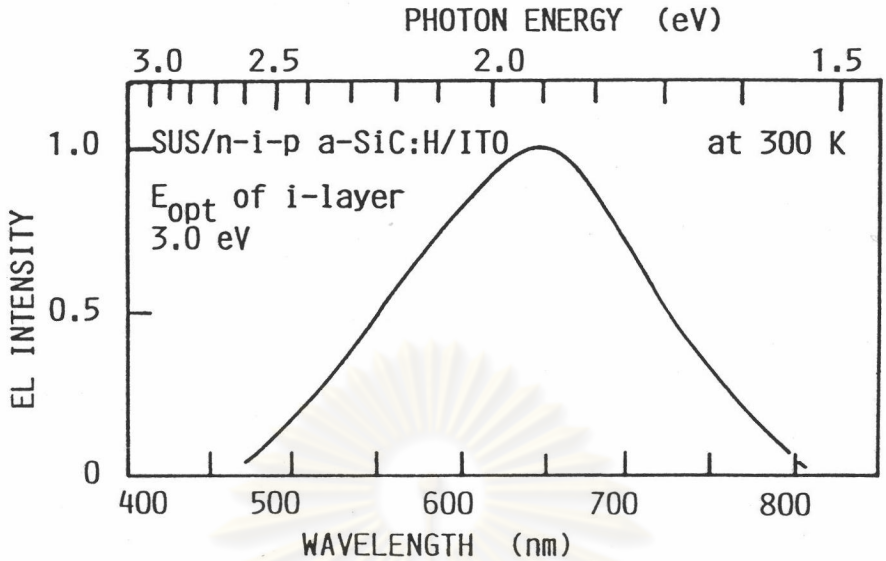

Figure 6.5 EL spectrum of a-SiC:H TFLED (E_{opt} of i-layer = 3.0 eV) deposited on a SUS substrate.

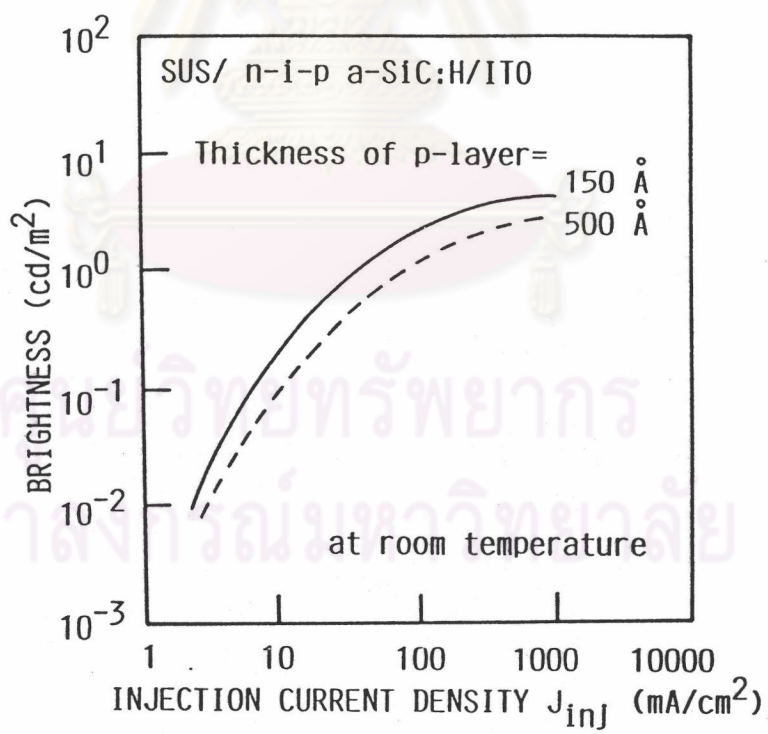

Figure 6.6 Comparison of the effect of the thickness of the top p-layer on the brightness for the case of the a-SiC:H TFLEDs deposited on SUS substrates.

Figure 6.6 shows a comparison of the effect of the thickness of the top p-layer on the brightness for the case of the TFLEDs having SUS substrates. It is found that the thinner p-layer results in higher brightness, because as the thickness of the p-layer increases, more light emitted from the i-layer will be absorpted in the p-layer.

Figure 6.7 shows the comparison of the brightness on the electrical power density consumed (J x V) for the TFLEDs deposited on a SUS substrate and on a glass substrate. It is seen that to obtain the same brightness the consumption of the electrical power density for the TFLED deposited on a SUS substrate is lower than for that deposited on a glass substrate. Since the lower electrical power consumption will generate less heat in the TFLED, therefore the brightness of the TFLED deposited on a SUS substrate should be higher than that deposited on a glass substrate.

The results from the above examination showed that at room temperature:

1) The threshold current necessary for the observation of the emission from the TFLED deposited on a SUS substrate is half of that from the TFLED deposited on a glass substrate.

2) The highest brightness is about 5 cd/m^2 for a SUS substrate while about 1 cd/m^2 for a glass substrate.

Table 6.1 shows thermal conductivity coefficient of glass and various kinds of metals. It is shown in this table that the thermal conductivity of a SUS material (0.96 W/m.K) is higher than that of a glass material (0.5 - 0.6 W/m.K) by a factor of about 1.5. However, the improvement of the brightness by using a SUS substrate as compared with a glass substrate resulted in a factor of about 2-5. It is interpreted that the increase of the brightness in the TFLED having SUS as a substrate should in some parts arise from the enhancement of the internal quantum luminescent efficiency due to the better thermal dissipation of the SUS material (heat sink effect) and in another part is due to a better back mirror effect from the excellent smoothness of the surface of the SUS substrate employed in the work. Further explanations of these effects are schematically illustrated in Fig. 6.8.

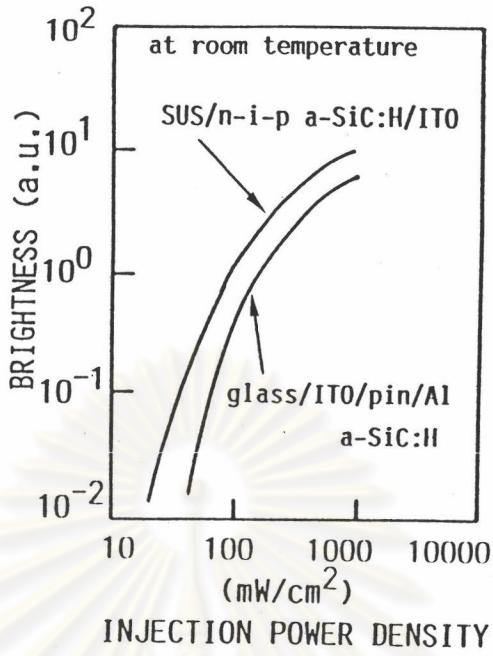

Figure 6.7 Comparison of dependences of the brightnesses on the electrical power density consumed (J x V) in the TFLEDs deposited on a SUS substrate and on a glass substrate.

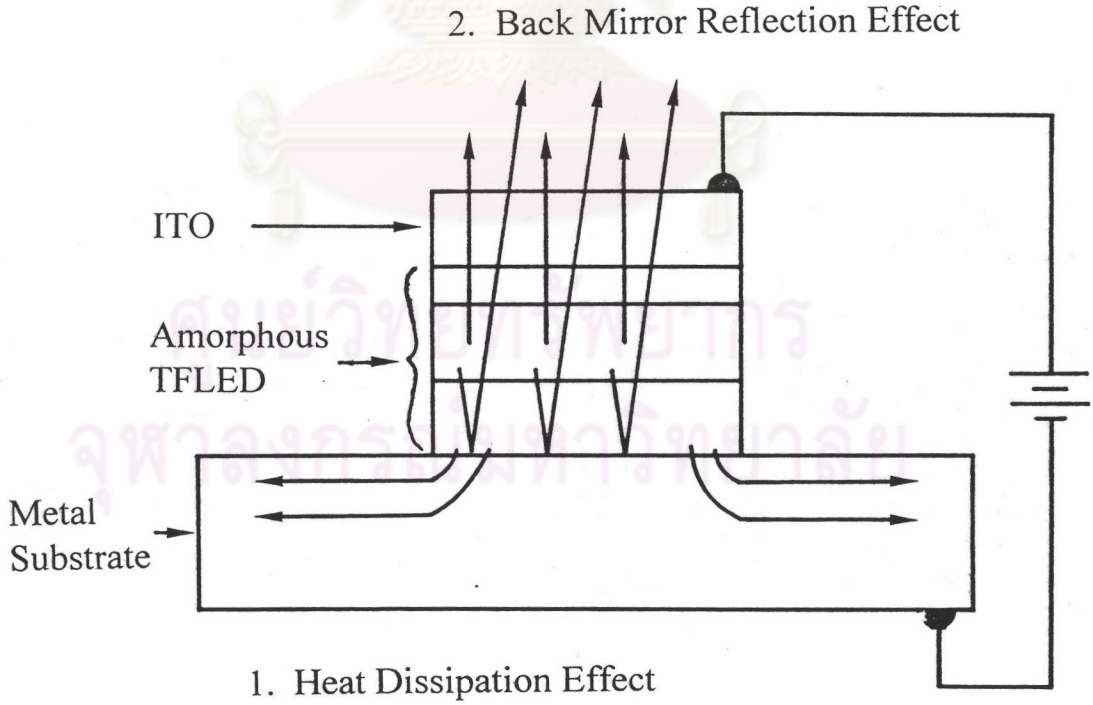

Figure 6.8 Schematic illustration of thermal dissipation and back mirror effects in amorphous TFLED deposited on a metal substrate

Table 6.1 Thermal conductivity coefficient of glass and various kinds of metals.

Materials	Thermal Conductivity Coefficient (W/m.k) measured at room temperature
SiO_2	0.69
Ag	23.0
Cu	22.2
Al	12.4
W	9.4
Zn	6.45
Fe	4.06
Ti	1.0
Si	2.0
SUS (Stainless steel)	0.96

It is well known that SUS material is more stable to the bombardment of plasma than Al and Ag metals, while Al and Ag have better thermal conductivities (12 and 23 W/m.K, respectively). Therefore, if the problem of atomic interdiffusions from Al, Ag sheets due to plasma is solved, a brighter TFLED deposited on Al, Ag sheet might be expected.

There is a direct evidence that the brightness of an a-SiC:H TFLED depends on the measured temperature as shown in Fig. 6.9 [9-10]. It is seen in the figure that the brightness of an a-SiC:H TFLED decreases as the temperature of the device increases. The result was interpreted as due to the decrease in the radiative recombination efficiency and carriers are thermally excited from the gap states to the extended states as the temperature increases. These data support the experimental results in Fig. 6.4 related to the increase in the brightness of the a-SiC:H TFLED deposited on a metal substrate. In other words, the heat sink or thermal dissipation effect by the metal substrate contributes to the improvement of the brigntess of the TFLED.

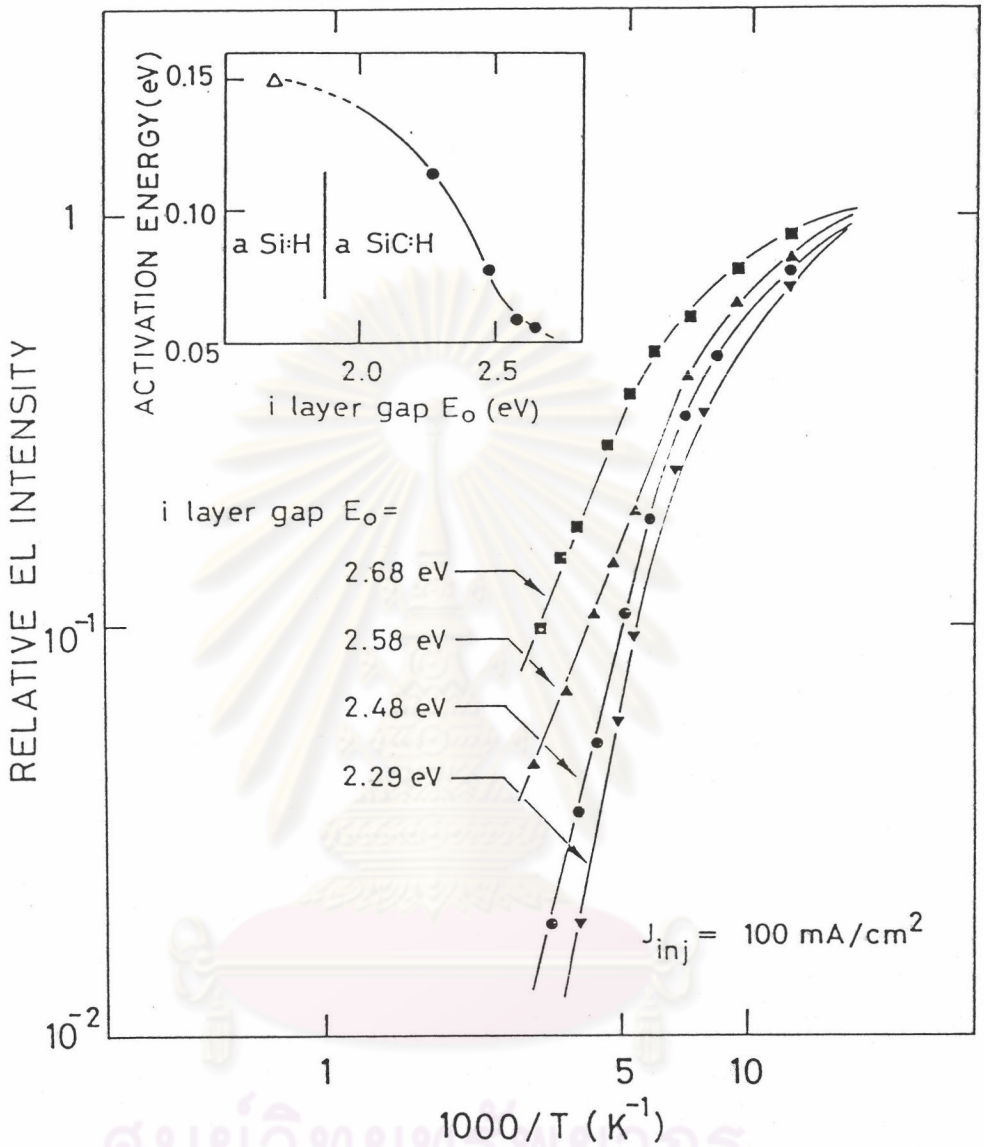

Figure 6.9 Relation between the EL intensity and the reciprocal of the measured temperature of TFLEDs. The parameter is the optical energy of the i-layer. The intensity of each TFLED is normalized to the same magnitude at 77 K [9-10]

6.2.4 Demonstrations of Actual Emissions from a-SiC:H TFLEDs with Metal Substrates

The emitting pattern in the TFLED having metal sheet as a substrate can be realized by either depositing the top transparent electrode having a desired pattern, or by inserting an insulating thin film in between the TFLED and the metal substrate.

Figure 6.10 shows the photographs of a-SiC:H TFLEDs deposited on various kinds of metal substrate, e.g., SUS, Cu, Al, Zn. The emitting pattern is determined by the pattern of the top ITO electrode.

Figure 6.11 shows a photograph of an actual emission (size 3 x 3 mm^2) from an orange-red a-SiC:H TFLED having SUS as a substrate. The black shade in the picture is the front probe.

Figure 6.12 shows a photograph of an actual emission (size 3 x 3 mm^2) from a yellow a-SiC:H TFLED having SUS as a substrate. The black shade in the picture is the front probe.

Another method to get a desired emitting pattern is to deposit an insulating layer onto specified locations of the metal substrate before the deposition of the p-i-n amorphous layers as shown in Fig. 6.13. Figure 6.13 shows the deposition of an insulating layers onto specified locations of a metal substrate in advance to the deposition of the p-i-n amorphous layers. The emission will be observed from the locations where the insulating layers do not exist.

A moving emitting pattern can be obtained in the TFLED with a metal substrate by using the matrix configuration proposed in Fig. 6.14. Figure 6.14 shows a structure of a moving emitting pattern of the a-SiC:H TFLED with a metal substrate. First, an insulating layer was deposited on the whole area of a metal substrate, followed with the deposition of grid conductive electrodes (ITO, Al, etc.). Next the p-i-n amorphous layers were deposited on the whole area. Finally, grid ITO electrodes were deposited on the top.

It has been pointed out in this section that the surface of the metal substrate has to be very smooth (typically less than 0.1 micron). We have found that we can solve the problem in the case when we have to use a rough surface substrate. As is

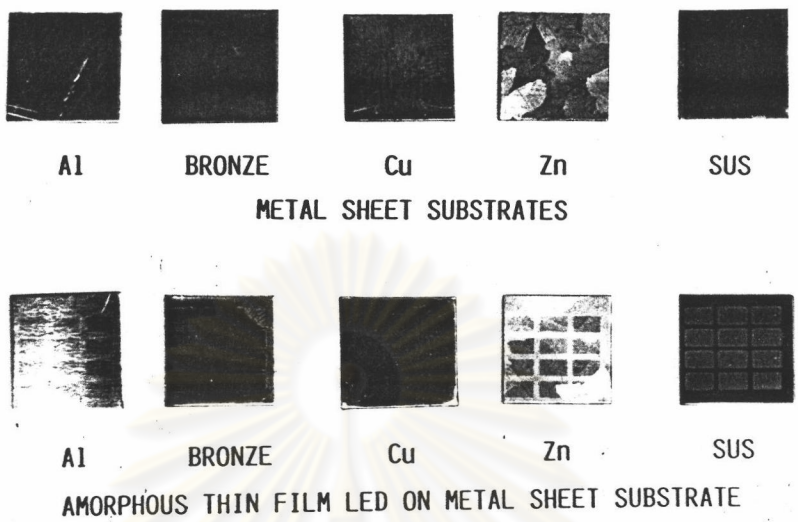

Figure 6.10 Photographs of a-SiC:H TFLEDs deposited on various kinds of metal substrates, e.g., SUS, Cu, Al, Zn.

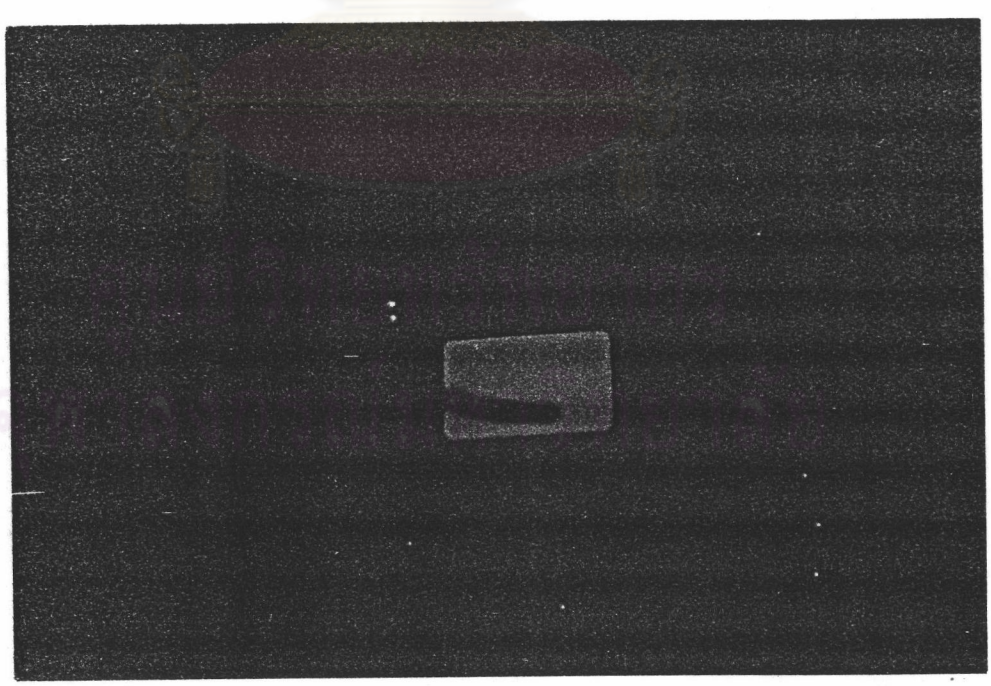

Figure 6.11 Photograph of an actual emission (size 3 x 3 mm^2) from an orange-red a-SiC:H TFLED deposited on a SUS substrate.

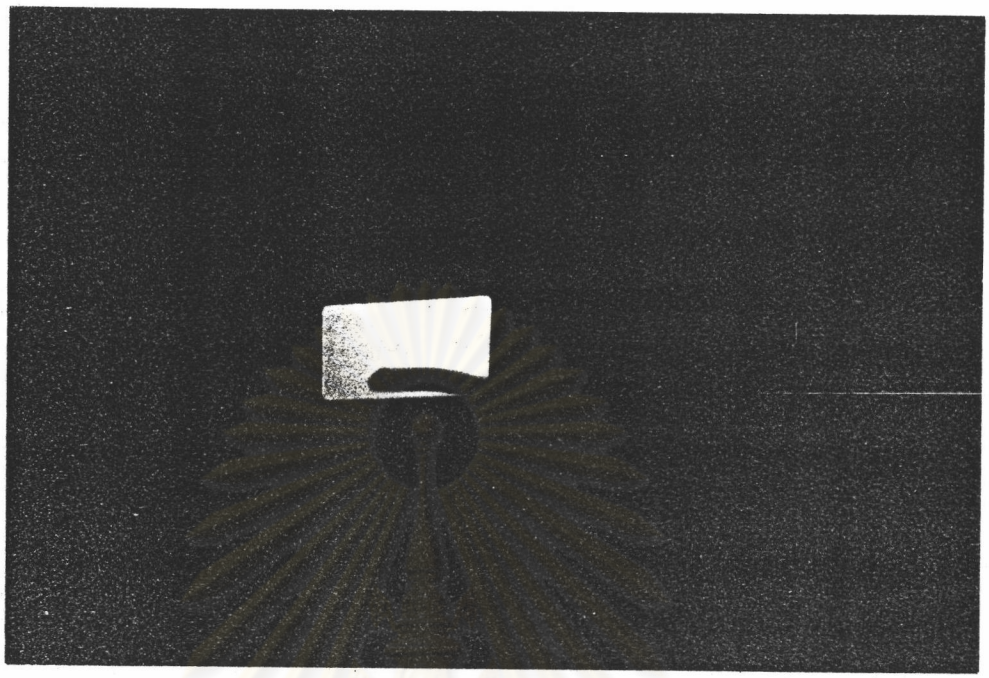

Figure 6.12 Photograph of an actual emission (size 3 x 3 mm^2) from a yellow a-SiC:H TFLED deposited on a SUS substrate.

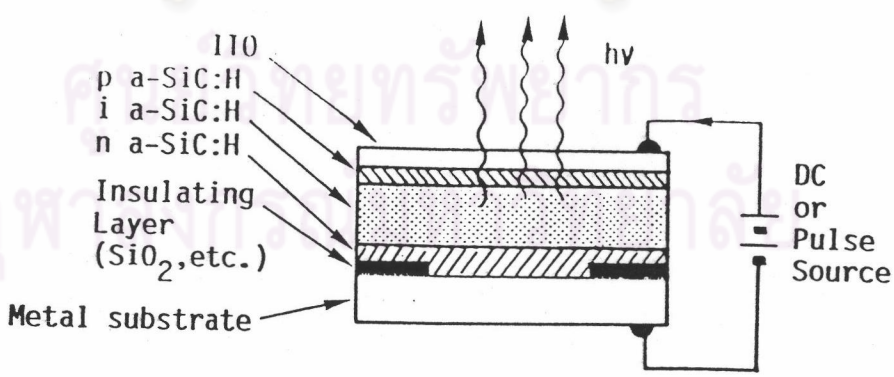

Figure 6.13 Deposition of insulating layers onto specified locations of a metal substrate in advance to the deposition of the p-i-n amorphous layers.

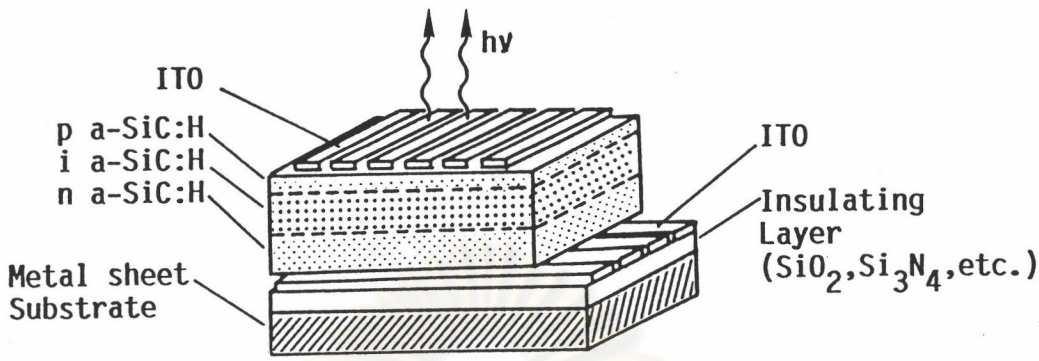

Figure 6.14 Structure of a moving emitting pattern of the a-SiC:H TFLED with a metal substrate.

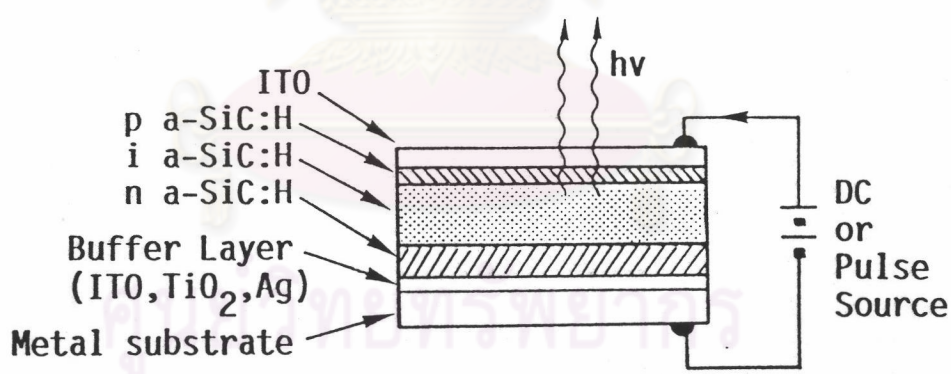

Figure 6.15 Structure of the a-SiC:H TFLED using a buffer conductive layer before the deposition of p-i-n amorphous layers on a metal substrate.

shown in Fig. 6.15, it will be very effective if one deposits a buffer conductive layer, for example ITO, TiO_2 and Ag before the deposition of the p-i-n amorphous layers.

6.3 Improvement of Brightness by Using Boron Doped Highly Conductive and Wide Gap a-SiO:H and μc-SiO:H as p-layer

In this section another effort to improve the brightness of an amorphous TFLED has been done by focusing on the improvement of the hole injection efficiency from the p-layer into the i-layer. The material used as the p-layer in this work has been restricted to p-a-SiC:H so far. The drawback of the p-a-SiC:H is the limitation of the optical energy gap as small as 2.0 eV and the conductivity is as low as 10^{-7}-10^{-8} S/cm. In order to get hole injection efficiency, one needs a wider and higher conductive p-type materials.

Recently, Fuji Electric group reported that boron doped highly conductive and wide bang gap amorphous silicon oxide (p-a-SiO:H) and microcrystalline silicon oxide (p-μc-SiO:H) can be prepared by the conventional glow discharge plasma CVD method [11-12], and the materials are useful in the improvement of the performances of a-Si:H solar cell.

It this work the author has succeeded in the application of the p-a-SiO:H and p-μc-SiO:H to the p-layer in high efficiency amorphous TFLED. The project was resulted from the collaboration between the Fuji Electric group and the author [3]. First, the glass/ITO/ p-SiO:H samples were prepared at Fuji Electric Corporate R&D Ltd. in Japan, then the samples were sent to Thailand. Next the i-a-SiC:H/ n-a-SiC:H/Al layers were deposited by the author in Thailand.

In this section a series of results of experiments on the preparation of p-a-SiO:H and p-μc-SiO:H and the application of these materials to the p-layer in amorphous TFLED are described and discussed.

6.3.1 Preparation and Basic Properties of p-a-SiO:H and p-μc-SiO:H Films

The p-a-SiO:H and p-μc-SiO:H films were deposited by the glow discharge plasma RF (13.56 MHz) method from a gas mixture of SiH_4 + CO_2 + H_2. The details

have been reported in the literatures [11-12]. The unique know-how of the preparation is the high hydrogen as dilution during the deposited and the high RF power density. The films were deposited under appropriate conditions where the hydrogen dilution ratio (H_2 / SiH_4) ranged from 10 to 30. Table 6.2 shows typical preparation conditions for p-a-SiO:H and p-μc-SiO:H.

Table 6.2 Typical preparation conditions for p-a-SiO:H and p-μc-SiO:H.

$CO_2/(SiH_4+CO_2)$	0-0.6
H_2/SiH_4	160-320
B_2H_6/SiH_4	06-1.0%
Substrate Temperature	100-250 °C
Pressure	1.0 Torr
RF Power Density	5-50 mW/cm^2.

It was reported that the films contain Si, H and O atoms. The content of the C atom was so small that it was under the detection limitation of ESCA.

Figure 6.16 shows the effect of the gas ratio, $CO_2/(SiH_4+CO_2)$, on the optical gap, dark conductivity and photoconductivity of p-type μc-SiO:H [11]. The conductivity decreases with increases in the gas ratio while the optical gap increases due to the incorporation of oxygen into the film.

Figure 6.17 shows the photo-and dark conductivity of boron doped a-SiO:H and μc-SiO:H as a function of the optical gap [11]. As can be seen from this figure, the conductivities of p-μc-SiO:H are about four orders of magnitude higher than those of conventional p-a-SiO:H in the optical gap range of 2.15-2.25 eV. The reason why μc-SiO:H films have higher conductivities than a-SiO:H films seems to be the fact that they include a conductive microcrystalline phase. At this stage, we believe that the p-μc-SiO:H is a promising material for not only the window layer of a-SiH solar cells but also the hole injector layer in the amorphous TFLEDs.

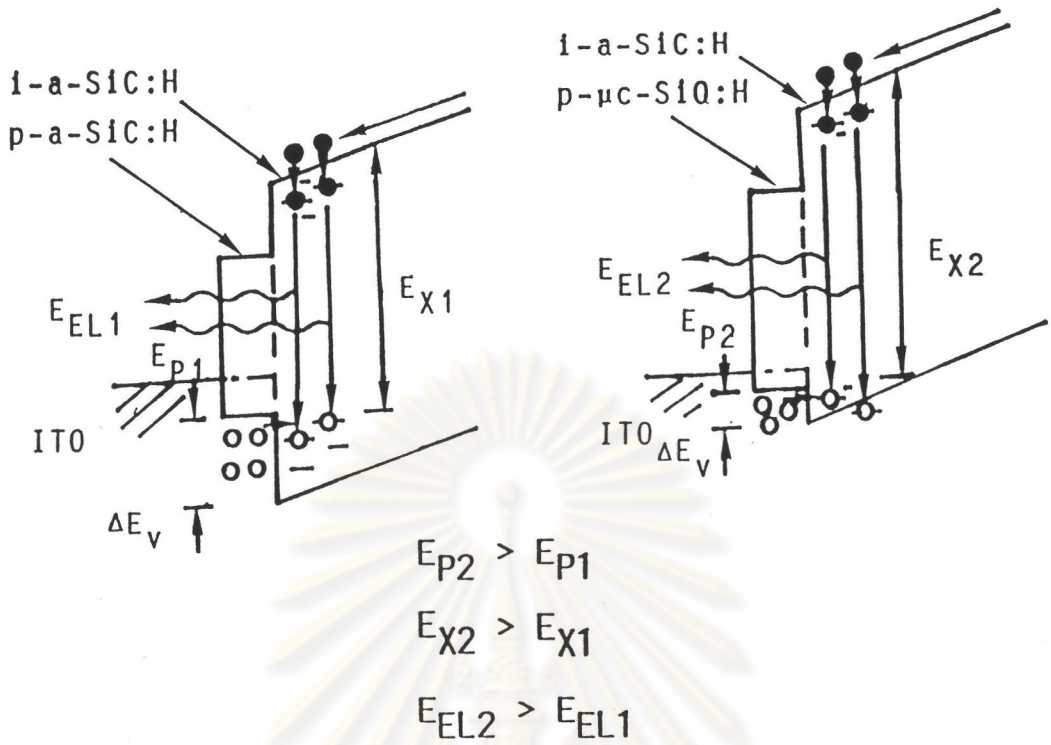

Figure 6.21 Band diagrams of the amorphous TFLED at the vicinity of p/i interface with different optical energy gaps of the p-layer.

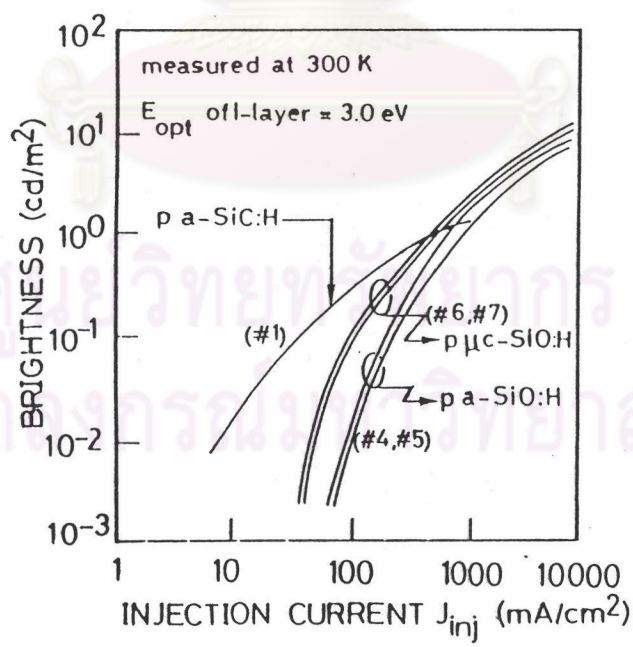

Figure 6.22 Comparison of the brightnesses of the a-SiC:H TFLEDs which have different materials of the p-layers.

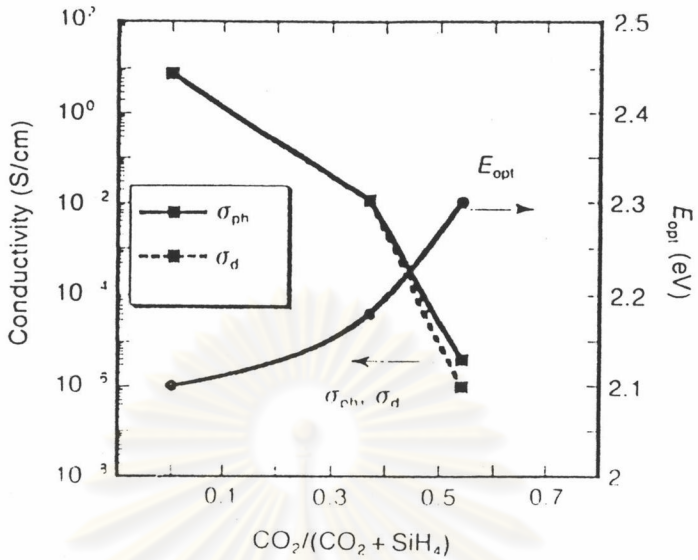

Figure 6.16 Effect of the $CO_2/(SiH_4+CO_2)$ gas fraction on the optical gap, dark conductivity and photoconductivity of p-type μc-SiO:H [11].

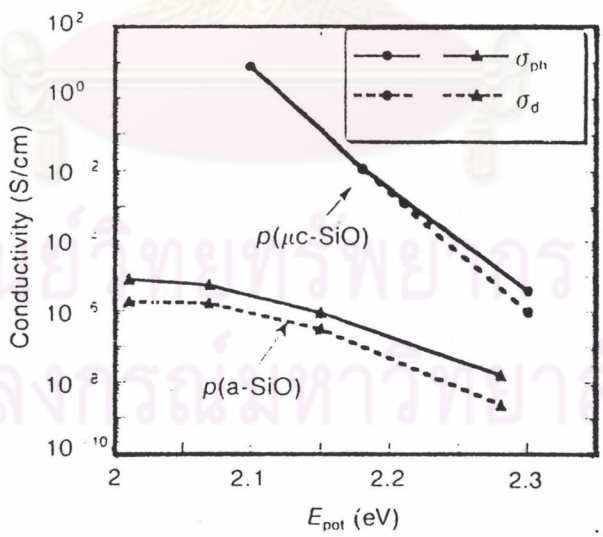

Figure 6.17 Photo-and dark conductivity of boron doped a-SiO:H and μc-SiO:H as a function of the optical gap [11].

6.3.2 Fabrication and Characteristics of p-a(μc)-SiO:H/i-a-SiC:H/n-a-SiC:H TFLED

As described in previous section, the highly-conductive and wide band gap p-type a-SiO:H and μc-SiO:H can be prepared by glow discharge plasma CVD method. The conductivities of the p a-SiO:H and μc-SiO:H are in the range of 10^{-6} - 10^{-8} S/cm. The optical energy gaps are in the range of 2.15 - 2.40 eV.

Figures 6.18 (a) - (e) show various structures of the amorphous TFLEDs developed so far in this work. The devices that contain the p-a-SiO:H and p-μc-SiO:H as the p-layers are shown in Fig.6.18 (d) and (e), respectively.

The device (d) has a structure of glass/ITO/p-a-SiO:H/i-a-SiC:H/n-a-SiC:H/Al.

The device (e) has a structure of glass/ITO/p-μc-SiO:H/i-a-SiC:H/n-a-SiC:H/ Al.

Table 6.3 shows the detailed parameters of various structures and various samples of TFLEDs. In this section we will emphasize on the structures (d) and (e) (samples #4, #5, #6 and #7).

The TFLED samples #4 and #5 have p-a-SiO:H as the p-layers. The TFLED samples #6 and #7 have p-μc-SiO:H as the p-layers in the TFLEDs.

Figure 6.19 shows electroluminescent spectra for the TFLEDs have different p-layers. The materials of the i- and n-layers are i-a-SiC:H (3.0 eV) and n-a-SiC:H (2.0 eV). The optical energy gap of p-a-SiC:H (sample #1) is 2.0 eV. The optical energy gaps of p-a-SiO:H (sample #4, #5) are 2.15 and 2.30 eV. The optical energy gaps of p-μc-SiO:H (sample #6,#7) are 2.30 and 2.40 eV.

It is found in Fig. 6.19 that, with increase in the optical energy gap of the p-layer, the EL spectrum moves towards higher photon energy. Figure 6.20 summarizes the dependence of the peak of the EL spectrum on the optical energy gap of the p-layer. As the optical energy gap of the p-layer increases from 2.0 eV to 2.40 eV, the peak of the EL spectrum moves from 1.83 eV to about 2.10 eV.

The shift of the EL spectrum with the optical energy gap of the p-layer can be explained as follows (see Fig. 6.21):

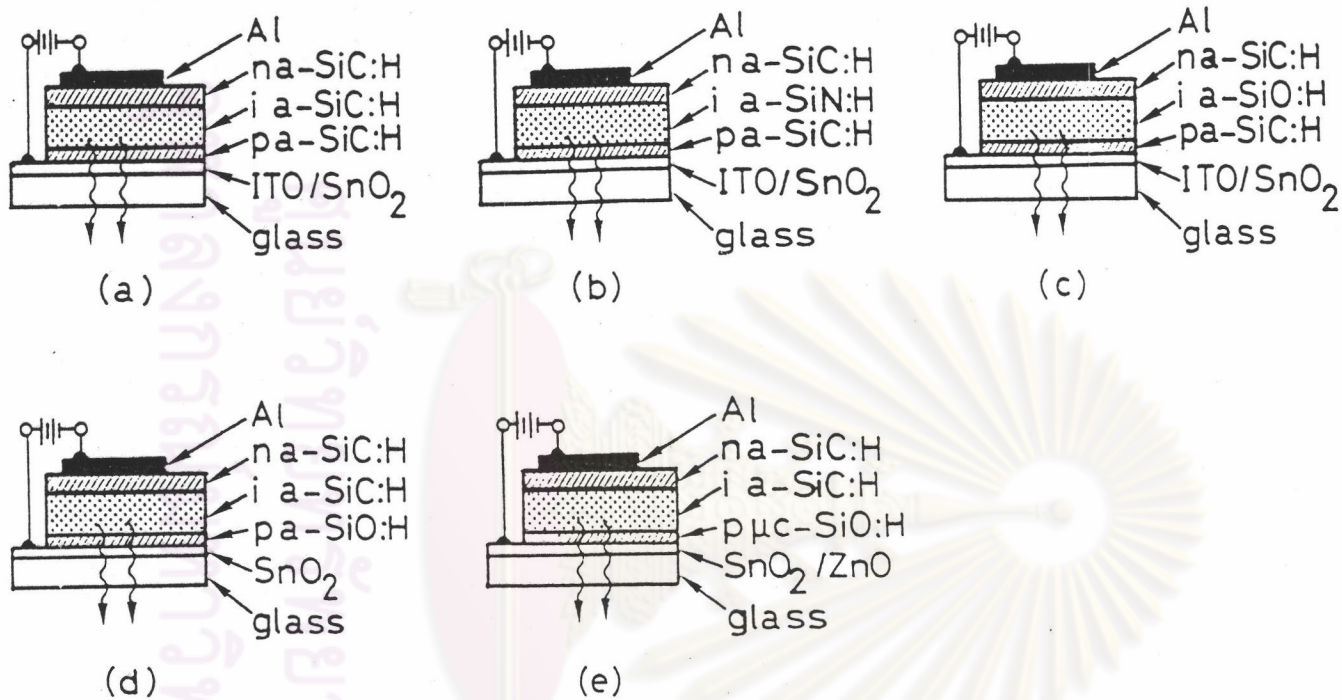

Figures 6.18 Various structures of the amorphous TFLEDs fabricated in this work.

(a) glass/ITO/p-a-SiC:H/i-a-SiC:H/n-a-SiC:H/Al.

(b) glass/ITO/p-a-SiC:H/i-a-SiN:H/n-a-SiC:H/Al.

(c) glass/ITO/p-a-SiC:H/i-a-SiO:H/n-a-SiC:H/Al.

(d) glass/ITO/p-a-SiO:H/i-a-SiC:H/n-a-SiC:H/Al.

(e) glass/ITO/p-μc-SiO:H/i-a-SiC:H/n-a-SiC:H/Al.

Table 6.3 Detailed parameters of various structures and various samples of TFLEDs.

Type	Sample No.	TCO Materials	p-layer	i-layer	n-layer
(a)	#1	ITO/SnO_2 (1800Å/200Å)	a-SiC:H (2.0 eV, 150 Å)	a-SiC:H (3.0 eV, 500 Å)	a-SiC:H (2.0 eV, 500 Å)
(b)	#2	ITO/SnO_2 (1800Å/200Å)	a-SiC:H (2.0 eV, 150 Å)	a-SiC:H (3.0 eV, 500 Å)	a-SiC:H (2.0 eV, 500 Å)
(c)	#3	ITO/SnO_2 (1800Å/200Å)	a-SiC:H (2.0 eV, 150 Å)	a-SiC:H (3.0 eV, 500 Å)	a-SiC:H (2.0 eV, 500 Å)
(d)	#4	SnO_2 (9000Å)	a-SiO:H (2.15 eV, 500 Å)	a-SiC:H (3.0 eV, 500 Å)	a-SiC:H (2.0 eV, 500 Å)
(d)	#5	SnO_2 (9000Å)	a-SiO:H (2.3 eV, 120 Å)	a-SiC:H (3.0 eV, 500 Å)	a-SiC:H (2.0 eV, 500 Å)
(e)	#6	SnO_2 /ZnO (9000Å/300Å)	μc-SiO:H (2.3 eV, 200 Å)	a-SiC:H (3.0 eV, 500 Å)	a-SiC:H (2.0 eV, 500 Å)
(e)	#7	SnO_2 /ZnO (9000Å/300Å)	μc-SiO:H (2.4 eV, 200 Å)	a-SiC:H (3.0 eV, 500 Å)	a-SiC:H (2.0 eV, 500 Å)

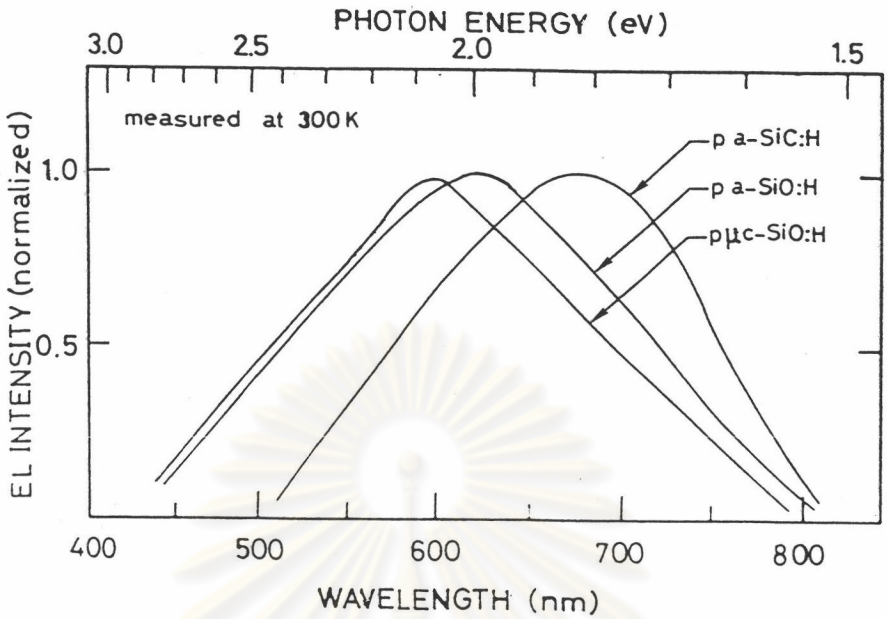

Figure 6.19 EL spectra for a-SiC:H TFLEDs having different p-layers.

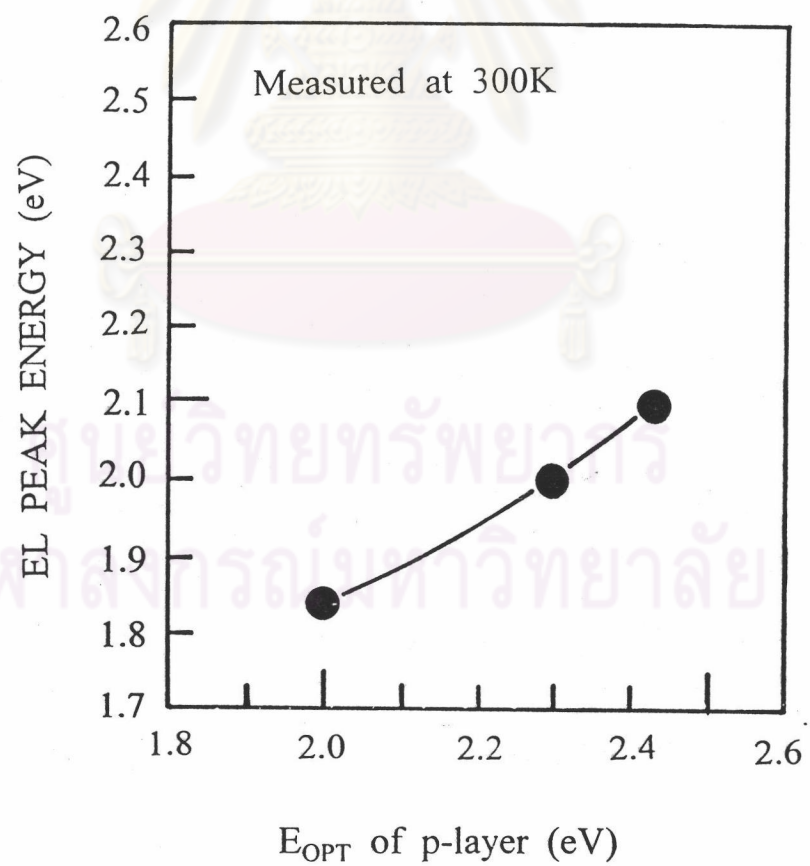

Figure 6.20 Dependence of the peak energy of the EL spectrum on the optical energy gaps of the p-layer.

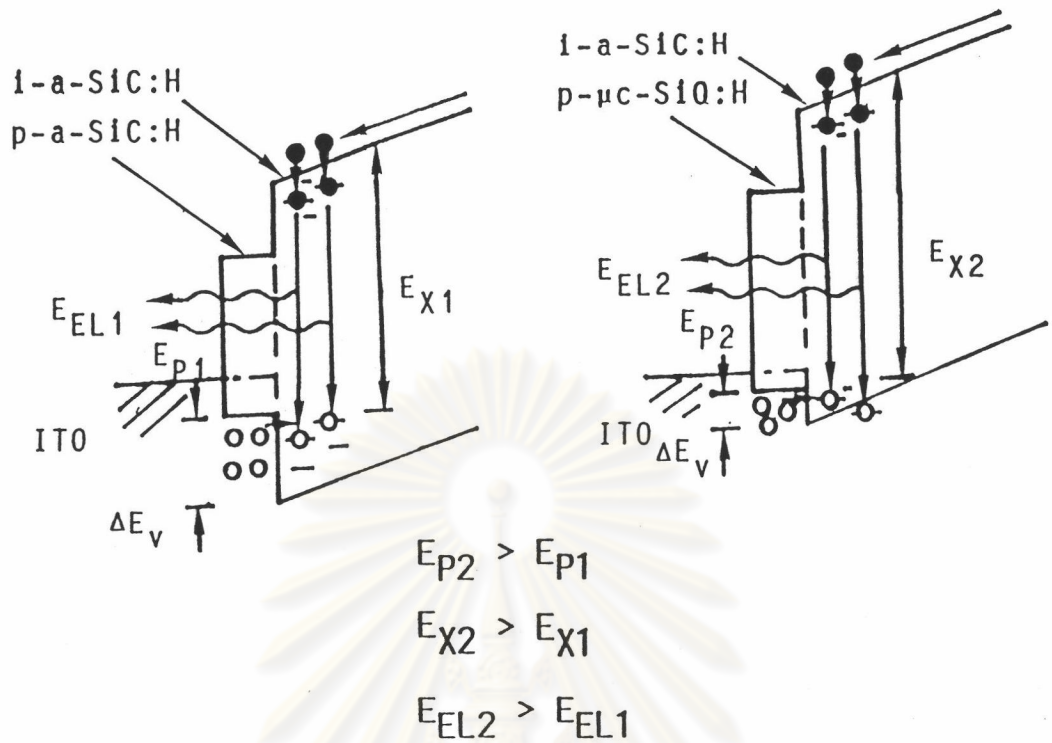

Figure 6.21 Band diagrams of the amorphous TFLED at the vicinity of p/i interface with different optical energy gaps of the p-layer.

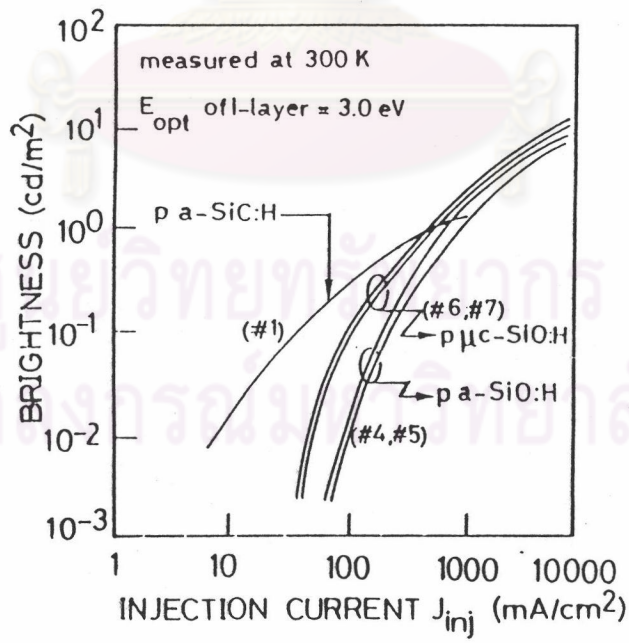

Figure 6.22 Comparison of the brightnesses of the a-SiC:H TFLEDs which have different materials of the p-layers.

It has been clarified in chapters 3-5 that the carrier injection in the amorphous silicon alloy TFLED is based upon the tunneling of holes and electrons through the notch barriers at the p/i and i/n interfaces, respectively. Holes seems to be injected into the deep localized states at the valence band side and recombined with electrons before holes can thermally excited down to the valence band edge. In this situation,

1. If the optical energy gap of the p-layers ($E_{p2} > E_{p1}$) increases, the excitation energy level of holes will increases ($E_{x2} > E_{x1}$).

2. When the excitation energy level of holes increases ($E_{x2} > E_{x1}$), the EL spectrum will peak at higher energy region.

It is concluded here that the p-a-SiO:H and p-μc-SiO:H are useful in the blue shift of the EL spectrum of the amorphous TFLED.

Figure 6.22 shows the comparison of the brightnesses of the TFLEDs which have different materials of the p-layers. The sample #1 has the conventional p-a-SiC:H layer, the samples #4, #5 have the new p-a-SiO:H layer and the samples #6, #7 have the new p-μc-SiO:H layers. It is seen in this figure that the brightnesses of the TFLEDs are improved to the level of 10 cd/m^2 by using the new materials; p-a-SiO:H and p-μc-SiO:H. The increase in the brightness with the increase in the optical energy gap of the p-layer can be interpreted as due the improvement of the injection efficiency as well as the injection energy level of holes.

6.4 Summary

The improvements of the brightness of the amorphous TFLED have been successfully done. The first effort is to improve the internal luminescent efficiency by controlling the temperature of the TFLED by using a metal substrate. The metal substrate has a better thermal conductivity coefficient so that heat generated in the TFLED can be quickly dissipated to the ambient. By this technique the brightness has been increased by a factor of 2-5 to the level of 5 cd/m^2. Moreover, metal substrates also have various advantages, e.g., they are flexible, they are conductive electrodes by themselves, they are rigid, not broken, they are heat sink by themselves, etc. A patent on this subject has been applied [8].

The second effort to improve the brightness has been done by improving the hole injection efficiency by using new materials, so-called p-type amorphous silicon oxide (p-a-SiO:H) and p-type microcystalline silicon oxide (p-μc-SiO:H). The materials have wider optical energy gaps and higher conductivities than those of conventional p-a-SiC:H. By using these excellent materials not only the EL spectrum shifts to higher energy but also the brightness is increased to the level of 10 cd/m^2. This is the best record reported so far.

References

1. Boonkosum, W., Kruangam, D., and Panyakeow, S. Amorphous visible-light thin film light-emitting diode having a-SiN:H as a luminescent layer. Jpn. J. Appl. Phys. 32 No. 4 (April 1993) : 1534-1538.
2. Boonkosum, W., DeLong, B., Kruangam, D., and Panyakeow, S. Novel visible amorphous silicon carbide thin film LED. The 1st International Symposium on Laser and Optoelectronics Technology and Applications (ISLOE). Singapore. (November 11-14, 1993) : 300-305.
3. Boonkosum, W., Kruangam, D., Ratvises, B., Sujaridchai, T., and Panyakeow, S. Visible amorphous SiO:H thin film light emitting diode. The 16th International Conference on Amorphous Semiconductors: Science and Technology (ICAS 16) Kobe. Japan. (September 4-8, 1995).
4. Hong, J.W., Jen, T.F., Shin, N.F., Ning, S.L., and Chang, C.Y. Amorphous-SiC thin film light emitting diode using quantum-well-injection structures. The 1992 Int. Conf. Solid State Devices & Materials. Tsukuba. Japan. (1992) : 382-384.
5. Lau, S.P., Marshall, J.M., Dyer, T.E., Hepburn, A.R., and Davies, J.F. a-SiC:H thin film visible light emitting diode with highly conductive wide band gap a-SiC:H as the carrier injection layer. J. Non-Crys. Sol.164-166 (1993) : 813-816.
6. Paasche, S.M., Toyama, T., Okamoto, H., amd Hamakawa, Y. Amorphous SiC thin film p-i-n light emitting diode uisng amorphous SiN hot carrier tunneling injection layers. IEEE Trans. Electron Devices ED-36 (1989) : 2895-2902.
7. Boonkosum, W., Kruangam, D., DeLong, B., and Panyakeow, S. Improvement of brightness & threshold current in visible light a-SiC:H thin film LED by using metal sheet substrate. Mat. Res. Soc. Proc. Symp. 336 (1994) : 849-854.

8. Kruangam, D., Panyakeow, S., Sawadsaringkarn, M., Toprasertpong, B., Antarasena, C., Cholpranee, T., Sriyudthsak, M., Ratanathammaphan, S., Ratwiset, B., Thainoi, S., Boonkosum, W., and DeLong, B. Amorphous semiconductor thin film light emitting Diode", United State, Patent Application No. 08/414738 (1995).

9. Kruangam, D., Deguchi, M., Toyama, T., Okamoto, H. and Hamakawa, H. Carrier injection mechanism in a-SiC p-i-n junction thin film LED. IEEE Trans. Electron Devices ED-35 (1988) : 957 - 965.

10. Nonomura, S., Sakata, S., Kamada, T., Kida, H., Kruangam, D., Okamoto, H., and Hamakawa, Y. Detailed studies of optical edge and below gap absorption in a-$Si_{1-x}C_x$:H system. J Non-Crys. Solid. 77&78 (1985) : 865-868.

11. Fujikake, S., Ohta, H., Sichanugrist, P., Ohsawa, M., Ichikawa, Y., and Sakai, H. a-SiO:H films and their application to solar cells. Optoelectronic-Devices and Technologies. 9 (September 1994) : 379-390.

12. Sichanugrist, P., Sasaki, T., Asano, A., Ichikawa, Y., and Sakai, H. Amorphous silicon oxide and its application to metal/nip/ITO type a-Si solar cells. Technical Digest of the International PVSEC-7, Nagoya (1993) : 271-272.